Experiences with ultrasonic air mass flow rate measurement in gas turbine air intake ducts

A R Boucher*

**Real Time Power, Inc, Seestrasse 86, 8712 Stäfa, Switzerland, ray.boucher@realtimepower.net*

Keywords: air mass flow rate, gas turbine, ultrasonic.

Abstract

The air mass flow rate into the compressor of a gas turbine is a key parameter for determining and predicting the performance of combined cycle gas turbine (CCGT) power generation units. An accurate measurement of air flow rate can be used to improve the prediction of the gas turbine generator power output at the point when the exhaust gas temperature constraint is reached, and the subsequent calculation of thermal energy flow rate into the heat recovery steam generator (HRSG) improves the prediction of the steam turbine generator power output. The direct measurement of air mass flow rate is difficult because of the complex geometry of the air intake duct, and also because of the high levels of noise, vibration and air turbulence that are present. This paper will present the experiences gained from deploying a direct ultrasonic measurement of air speed in the intake duct, which is used in combination with static pressure measurements and the results of computational fluid dynamics (CFD) simulations to produce a real-time measurement of air mass flow rate. The challenges, accuracy and benefits of ultrasonic air mass flow rate measurement are discussed using experiences gained over the last six years from 28 field installations covering five different types of large (> 150 MW) industrial gas turbine.

1 Introduction

Since 2009, Real Time Power, Inc. have commissioned 28 ultrasonic air mass flow rate measurement systems in large industrial gas turbine air intake ducts. The gas turbine models concerned are W501F (8 installations), W501G (4 installations) and GT24 (14 installations). In addition, the system has been deployed at two gas turbine test facilities. In the majority of the installations, four ultrasonic probes have been mounted on the duct walls, usually in a plane on or close to the engine centre line. There are three installations where eight probes have been deployed in multiple planes.

Maximum air speeds and mass flow rates that have been measured by the systems are just over 50 m/s and just over 700 kg/s respectively (although not in the same installation). Ultrasonic probes have operated successfully within ducts for more than five years without the need for repair or replacement.

The measurement of air mass flow rate in a gas turbine intake duct using ultrasonic techniques presents particular challenges. Long straight passages of duct work are generally not encountered and therefore the only places where probes can be positioned are likely to be close to bends, tapering duct sections or restrictions – such as silencer baffles – and hence standard rectangular duct flow profiles cannot be assumed. In all installations to date, the probes have been located between the downstream end of the silencer baffles and the compressor bell mouth. At this region in the duct the ultrasonic noise levels coming from the compressor are around 20 times greater than the sound level of the received signals that are used to determine the air speed. This presents signal processing challenges in order to extract useful information from the noisy data. Vibration levels, especially in the inlet manifold, can interfere with the transducers, which have lightly damped resonant dynamics, and for this reason the probes are normally installed on the upstream side of the expansion joint between duct and manifold. Lastly, the flow is highly turbulent, with Reynolds numbers of 10^6 or higher, and hence the positions of sound paths must be carefully considered in order to minimize random uncertainty caused by air flow fluctuations.

The accuracy of the measurement will depend on the duct geometry and the air mass flow rate. Specifying the locations for the ultrasonic probes involves an engineering compromise between accuracy and signal strength, and also requires the consideration of mechanical constraints both inside and outside of the duct. An individual uncertainty analysis is required for each application after the post-installation survey is completed and initial test data have been recorded and compared to the CFD simulations. Typically a 1% (2σ) systematic uncertainty is obtained on the air mass flow rate reading, with lowest systematic uncertainties occurring at highest air speeds. The levels of random uncertainty caused by noise, vibration and turbulence are usually two to five times greater than the systematic uncertainty, and are greatest at highest air speeds. The use of adaptive model-based prediction techniques can be used to produce smoothed estimates of air speed and volumetric flow rate and thus reduce the impact of the random uncertainty on the computed mass flow rate.

This paper is organized as follows. Section 2 describes the principle of measurement. A worked example is presented in section 3 which illustrates how the systematic uncertainty of the measurement is calculated. The key points for installing

and commissioning an ultrasonic flow measurement are then summarized in section 4. The relationship to other gas turbine signals is discussed in section 5, and then validation techniques for the calculated air mass flow rate are presented in section 6. Notable experiences are presented in section 7, and finally conclusions in section 8.

2 Principle of measurement

The principle of measurement is the determination of the average air speed and speed of sound along two coplanar linearly independent vectors in the gas turbine air intake duct using the ultrasonic time-of-flight technique. A static pressure measurement also made at the same location in order that average air density and mass flux can be computed. Finally, CFD simulations are employed to determine the mathematical function relating the average air mass flux in the plane to the air mass flow rate in the whole duct. The following subsections outline the equations used in these three steps.

2.1 Air speed and speed of sound

Figure 1 presents the triangle of velocities that apply to an ultrasound pulse travelling from transmitter A to receiver B in a plane in a parallel-sided duct where s is the average air speed, and c is the average speed of sound. The path from A to B is set at an angle θ_{AB} with respect to the walls. The time of flight downwind from A to B is denoted by t_{AB}, the distance by AB and the ground speed $u_{AB} = AB/ t_{AB}$.

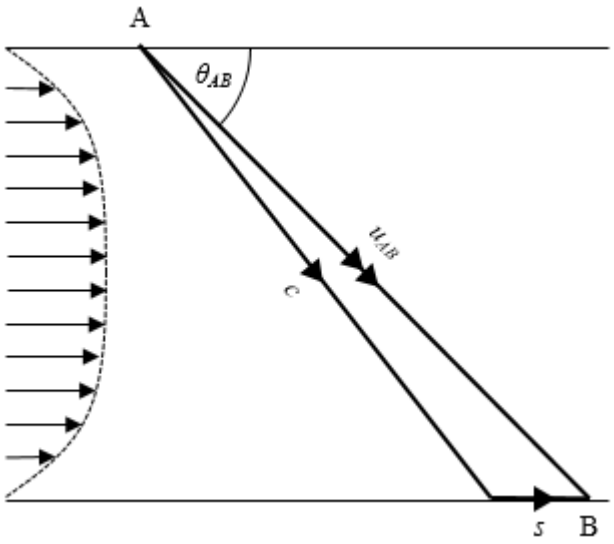

Figure 1: triangle of velocities.

From Figure 1, application of the cosine rule gives:

$$c^2 = {u_{AB}}^2 + s^2 - 2u_{AB}s.\cos\theta_{AB} \quad (1)$$

Similarly, by considering the time of flight of the ultrasound pulse in the upwind direction from B to A:

$$c^2 = {u_{BA}}^2 + s^2 + 2u_{BA}s.\cos\theta_{AB} \quad (2)$$

The elimination of c from Equations (1) and (2) gives the familiar result [1] for v_{AB}, the component of the air speed along the vector AB:

$$v_{AB} = s.\cos\theta_{AB} = \frac{AB}{2}\left(\frac{1}{t_{AB}} - \frac{1}{t_{BA}}\right) \quad (3)$$

Deriving this result from the triangle of velocities gives the correct equations for computing the speed of sound, which is obtained by back-substituting the value of s from Equation (3) into Equation (1) or (2). It should be noted that this assumes the component of s normal to the plane is zero. In practice this assumption is never true, but the effect of a nonzero component of s normal to the plane can be minimized by careful selection of the probe plane location, as discussed in section 4.

Even in the cases where the gas turbine air intake duct walls are parallel, it is often the case that the average air flow angle is not parallel to the walls, since long, straight sections of ducting are rarely encountered. For this reason, a second sound path, CD, is employed in order to obtain an estimate of the average air flow angle in the plane, θ, as well as the average air speed. This is illustrated in Figure 2 which shows a plan view of a trapezoidal duct section; a geometry that is present in 11 of the installed applications.

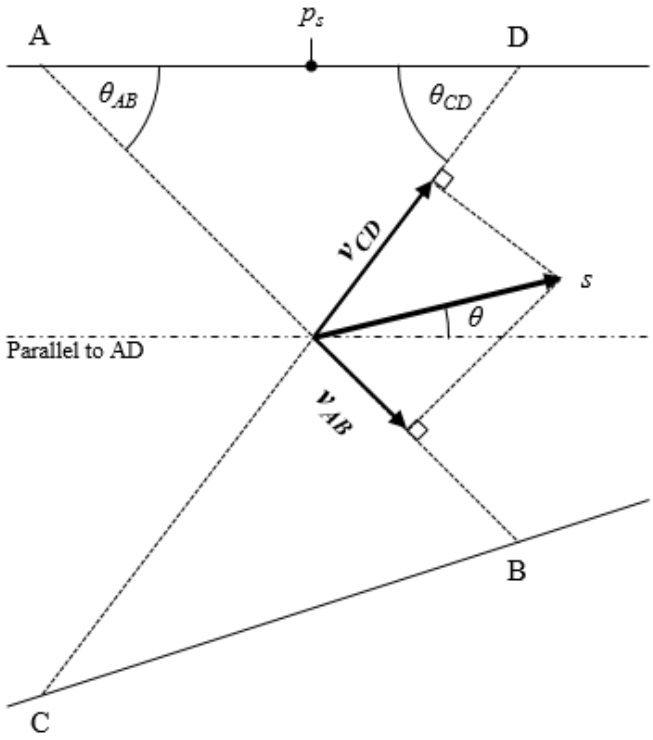

Figure 2: two sound paths in a trapezoidal duct.

From Figure 2, the application of triangle of velocities leads to Equations (4) and (5).

$$v_{AB} = s.\cos(\theta_{AB} + \theta) = \frac{AB}{2}\left(\frac{1}{t_{AB}} - \frac{1}{t_{BA}}\right) \quad (4)$$

$$v_{CD} = s.\cos(\theta_{CD} - \theta) = \frac{CD}{2}\left(\frac{1}{t_{CD}} - \frac{1}{t_{DC}}\right) \quad (5)$$

Expansion of the cosine terms and solution of the resulting two simultaneous equations, gives the following matrix equation for $s.cos\theta$ and $s.sin\theta$:

$$\begin{bmatrix} s.cos\theta \\ s.sin\theta \end{bmatrix} = \frac{1}{sin(\theta_{AB} + \theta_{CD})} \begin{bmatrix} sin\theta_{CD} & sin\theta_{AB} \\ -cos\theta_{CD} & cos\theta_{AB} \end{bmatrix} \begin{bmatrix} v_{AB} \\ v_{CD} \end{bmatrix} \quad (6)$$

From Equation (6), s and θ are straightforwardly derived as:

$$s = \sqrt{(s.cos\theta)^2 + (s.sin\theta)^2} \quad (7)$$

$$\theta = tan^{-1}(s.sin\theta / s.cos\theta) \quad (8)$$

These values of s and θ are then substituted into the following equations to determine the average speed of sound in the plane:

$$c_{AB}{}^2 = u_{AB}{}^2 + s^2 - 2u_{AB}s.\cos(\theta_{AB} + \theta) \quad (9)$$

$$c_{CD}{}^2 = u_{CD}{}^2 + s^2 - 2u_{CD}s.\cos(\theta_{CD} - \theta) \quad (10)$$

$$c^2 = (c_{AB}{}^2 + c_{CD}{}^2)/2 \quad (11)$$

It should be pointed out that the average air speed and flow angle values computed from Equations (4) to (11) are based only on two vector measurements and will not necessarily match the true average values for the whole of the plane bounded by ACBD in Figure 2. Any mismatch here is however accommodated by the same CFD simulation technique described in section 2.3.

2.2 Air density and mass flux

The average speed of sound in the plane can then be used in conjunction with a static pressure measurement, p_s, to calculate the average air density in the plane [2]:

$$\rho = \frac{\kappa p_s}{c^2} \quad (12)$$

where κ is the ratio of the specific heat capacities of air, for which a value of 1.4 is normally used, although this can be computed to greater accuracy if the moist air composition is known by making a measurement of relative humidity.

The average air mass flux (kg/s/m^2) in the plane is computed as the product of the average air density and the average air speed.

$$\dot{\bar{m}} = \rho s \quad (13)$$

2.3 Air mass flow rate

The air mass flow rate in the duct is then calculated as the product of the average air mass flux in the plane and the effective duct area A_{eff}.

$$\dot{m} = \dot{\bar{m}} A_{eff} \quad (14)$$

The effective duct area is computed using CFD simulations of the air flow in the duct at different mass flow rates and different air densities. In the simulations, the air mass flow rate and actual duct area are both known, and the simulated mass flow rate is then adjusted until the closest match is obtained with the air velocities v_{AB} and v_{CD} recorded in the measured data. The ratio of the effective area to the actual area is termed the *duct factor*, and is typically in the range 0.8 to 1.1, depending on where the plane of the ultrasonic transducers is located in relation to the fastest air speeds. The effective area will vary with air speed and/or speed of sound, and from the CFD simulations, a lookup table can be derived to compute A_{eff} from these measured values in real-time.

2.4 Update interval

The system has primarily been designed for making measurements at steady state flow conditions. The measurement rate is determined by the length of the sound paths, for example the time of flight on a 4 m sound path is around 11.7 ms at standard conditions. The controlling software then waits for a further three flight times before transmitting the next sound pulse in order to allow echoes to decay. This means each sound path would require 46.8 ms, and for a four probe system this would mean one new reading every 187.2 ms, or roughly 5 readings per second. This measurement rate will therefore impose an upper limit on the frequency of variations in air flow rate that can be detected.

3 Uncertainty analysis

The systematic uncertainty of the air mass flow rate measurement is dependent on the systematic uncertainties of following fundamental measurements of probe tip positions, tip-to-tip distances, and timings: A, B, C, D, *AB*, *CD*, t_{AB}, t_{BA}, t_{CD}, and t_{DC}. From these it is possible to calculate systematic uncertainties for the derived values of c, s and θ. Finally, the systematic uncertainty of the static pressure measurement and the duct factor are incorporated.

3.1 Positions, distances and timings

Three dimensional laser survey tools [3] are used post-installation to measure the ultrasonic probe tip coordinates *(x,y,z)* to an uncertainty of 1 mm (2σ) with reference to a datum point. The same tool can also scan the interior duct profile in three dimensions and permit cross sectional areas to be determined accurately. Hand-held laser distance measurement tools with 1 mm (2σ) uncertainty are also used to verify the tip-to-tip distances.

The timings are obtained from cross correlation of the actual and expected received signals. The transmitted sound pulses are swept sine waves, which are designed to produce a sharper correlation peak, and hence reduce jitter in the timing measurement. The expected received signals are computed

from the results of no-flow system identification tests which characterize the dynamics of each transmitter-receiver pair as two resonant second order transfer functions. Zero phase shift band pass digital filtering is employed to boost signal to noise ratios whilst preserving time of flight relationships. An oven controlled crystal oscillator (OCXO) provides a high stability external time base for the data acquisition card, and using this, the timing measurements have a 2σ uncertainty of 1 μs.

Monte Carlo analysis [4] is used to simulate measurement errors in the probe tip coordinates and also the timings at different air speeds and speeds of sound, and from this the standard uncertainties for c, s and θ can be obtained. A worked example is given here for illustration.

Duct dimensions: 3000 x 4000 mm
$AB = CD$ = 4000 mm
$\theta_{AB} = \theta_{CD}$ = 48.6 °
c = 345 m/s
s = 40 m/s
θ = 0 °

The uncertainties for c, s and θ from a Monte Carlo simulation of 1000 trials are presented to three decimal places in Table 1.

	σ	2σ	
c	0.031	0.062	m/s
s	0.013	0.027	m/s
θ	0.017	0.034	°

Table 1: systematic uncertainties for the worked example.

3.2 Static pressure and duct factor

A static pressure sensor with a 0.1% (2σ) accuracy is used.

The standard uncertainty of the duct factor is assigned from how closely the actual air velocity measurements are in agreement with the CFD predicted values. If a sufficiently fine, regular hexahedral mesh has been used, then typically the alignment between actual air velocities and CFD predicted value will be less than 0.5% of readings.

The worked example is continued in Table 2 using these additional pieces of information.

3.3 Additional uncertainty considerations

There may be other factors to consider when quantifying the uncertainty of the measurements. If the plane of the probes is oriented in the same way as the silencer baffles, and the upwind probes are close to the exit of the silencers, then small movements of the baffles, may have significant effects on the air speed that is being measured by the probes. CFD can be used to assess the sensitivity of the air speed measurement to the silencer baffle movement and an additional uncertainty introduced based upon this. In installations where the probe plane is perpendicular to the silencers this concern is not a problem.

The wind speed and direction outside of the air intake may cause the flow pattern inside the duct to change. This may be more pronounced on intake designs where there are three ports through which the air enters. The uncertainty due to wind effects can be reduced through the use of multiple probe planes. Only in 5 of the 28 installed systems are there such intakes with three entrance ports. The other 23 systems have intake ducts with a single port and no significant correlations between air flow pattern and wind speed and direction have yet been observed in these cases.

Variable	Value	Std. Uncert. (σ)	Eng. Units	2σ	2σ %
Air pressure	100000	50	Pa		
Speed of sound	345	0.031	m/s		
Air density	**1.1727**	**0.0006**	**kg/m^3**	**0.0012**	**0.11%**
Air density	1.1727	0.0006	kg/m^3		
Air speed	40	0.013	m/s		
Air mass flux	**46.91**	**0.03**	**kg/s/m^2**	**0.06**	**0.12%**
Duct minor dimension	3.000	0.002	m		
Duct major dimension	4.000	0.002	m		
Duct area	**12.000**	**0.010**	**m^2**	**0.02**	**0.17%**
Air mass flux	46.91	0.03	kg/s/m^2		
Duct area	12.000	0.010	m^2		
Duct factor	1.000	0.005			
Air mass flow rate	**562.9**	**2.9**	**kg/s**	**5.7**	**1.02%**

Table 2: air mass flow rate systematic uncertainty example.

4 Installation, commissioning and maintenance

This section summarizes experiences gained from installing, commissioning and maintaining the systems.

4.1 Installation

Choosing the best locations for the ultrasonic probes is crucial to obtaining best accuracy from the installed flow measurement system. There are several factors which must be considered in this process.

On an individual sound path, it is desirable to maximize the difference between the upwind and downwind times of flight.

This can be achieved by reducing the wall angle, however this will increase the path length, and therefore reduce the received signal strength. It is often the case that mechanical constraints, such as trash screens and expansion joints place a lower limit on the wall angle. With crossed sound paths, the optimum intersection angle is 90°. Again, it is normally mechanical constraints which prevent this angle from being achieved.

The other important factor for maximizing the timing differences is to place the plane of probes in the fastest flowing air. This will usually mean alignment with the centre line of the compressor. Sometimes this is not possible due to support struts, in which case the plane will need to be offset. As discussed in section 2.1 it is also desirable to locate the probe plane such that flow components normal to the plane are minimized, in order to reduce the uncertainty in the speed of sound measurement. This requirement is usually best satisfied by aligning the probe plane with the compressor centre line, but in situations where this is not possible, it may be achieved by rotating the plane. Once the plane of the probes has been specified, laser alignment tools are used to mark the intended probe positions and thus minimize deviations from the plane.

In deciding the probe locations, one must also consider the beam angles of the ultrasonic transducers and the drift that the sound pulses will experience at the highest flow rates. As a result, a pair of probes will not be aimed directly at each other, but rather the aiming point will be at an angle α upwind, as shown by point B* in Figure 3 and given by Equations (14) and (15). Aiming in this way will maximize the received signal strength at the highest flow rates. It will reduce the signal strength at lower flow rates, but at these conditions the noise levels are also lower, and the signal to noise ratio will therefore not be significantly diminished. For a pair of probes, the drift angle is the same in both upwind and downwind directions. Laser alignment tools are again used to ensure correct aiming.

$$\alpha_{AB} = sin^{-1}[(s/c)\sin(\theta_{AB} + \theta)] \quad (14)$$

$$\alpha_{CD} = sin^{-1}[(s/c)\sin(\theta_{CD} - \theta)] \quad (15)$$

The static pressure port should be located as close as possible to the plane as the probes, and to the intersection point of the crossed sound paths. If necessary, the port can be offset slightly above or below the probe plane so that it is clear from any wake of the upstream probe.

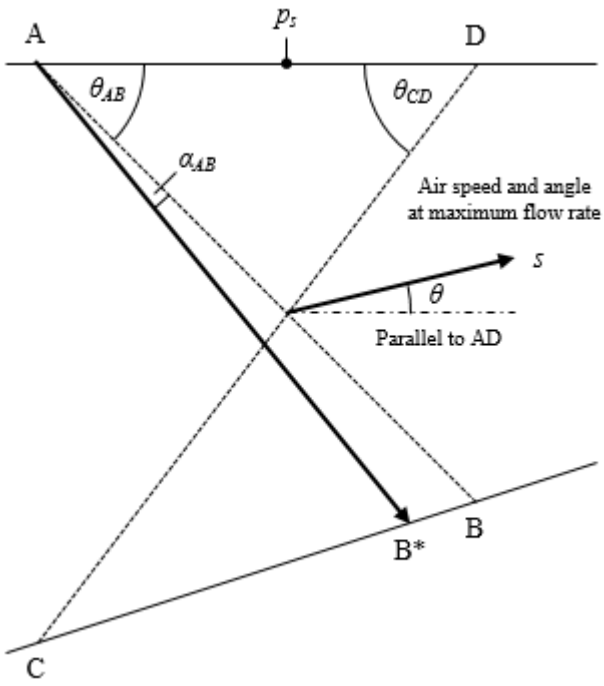

Figure 3: probe aiming to counteract drift at highest flow rates

4.2 Commissioning

The commissioning procedure after the probes have been installed and aimed involves a 3D laser survey to determine the probe tip coordinates with reference to a datum point in the duct. Laser distance measuring tools are also used to directly measure tip-to-tip distances and compare them with the 3D survey for quality control.

After the survey has been completed and while the engine is in a no-flow condition, system identification tests are performed on all sound paths to characterize the dynamics of the transmitting/receiving pair. These tuning settings are then configured in the system.

When the probe tip coordinates and tuning settings have been set, initial verification of the system can be performed by inspecting the speed of sound estimates from the two sound paths, and comparing these with the speed of sound computed from measurements of air pressure, relative humidity and temperature [5]. The numerical difference between c_{AB} and c_{CD} should normally be less than 0.5 m/s at no-flow conditions. Similar agreement should exist between the average speed of sound computed from the ultrasonic measurement and the value computed from the physical sensors.

Installation and commissioning will normally take between two and four days on-site, which means that it can comfortably completed within annual scheduled maintenance periods for the gas turbine.

4.3 Maintenance

Ultrasonic probes require little maintenance, since to some extent they are self-cleaning. The most significant unplanned maintenance events that have occurred with the measurement systems are listed here.

In one installation, an accumulation of chemical and biological material on the transducer faces attenuated the signal strength to an extent where the probe needed replacing. The probe in question was on the floor of the duct, facing upwind.

In another installation – in a vertical duct – upwind facing ultrasonic transducers failed electrically after the faces were struck by falling ice. The mechanically integrity of the transducer was not compromised in this event, but the ice did cause considerable damage in the initial compressor stages.

In a third installation, an upwind facing probe mounted on the side wall of a horizontal duct failed electrically after being struck by a foreign object. Once again, mechanical integrity of the probe was undiminished. Engine performance degradation was observed after this event and minor damage was found at a subsequent inspection.

5 Relationships to other gas turbine signals

At synchronous speed, the average air speed and volumetric flow rate readings are both highly correlated with the compressor inlet guide vane (IGV) angle. The strongest correlations are obtained in ducts where air flow patterns are least disturbed by support struts, and the ultrasonic probes are relatively far away from both the bell mouth and the silencer baffles. Figure 4 illustrates such a case, showing the high correlation between average air speed in the plane, *s*, and IGV angle over the full operational range of an engine from full-speed-no-load (FSNL) to base load.

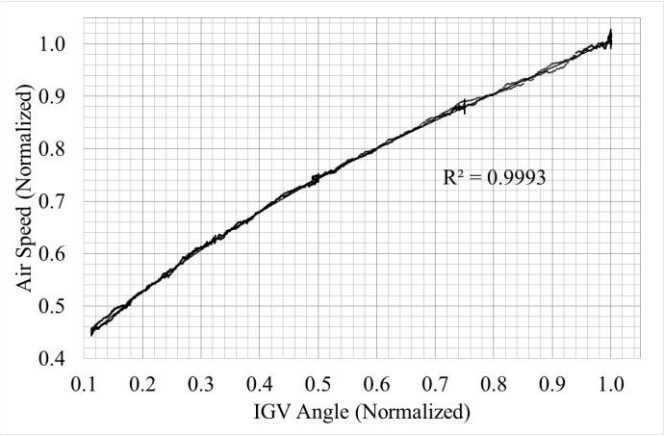

Figure 4: air speed vs IGV angle at synchronous speed

At shaft speeds less than synchronous speed, and with constant IGV angle, the air speed reading is strongly correlated with shaft speed, allowing the system to be used for measurements of air flow rate during start up and shutdown of the gas turbine. This is shown in Figure 5.

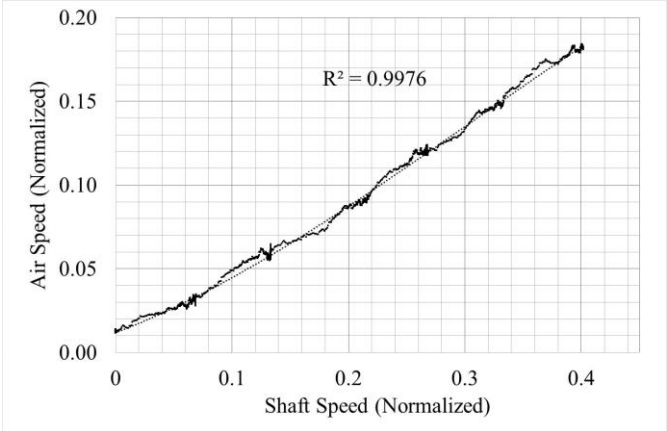

Figure 5: air speed vs shaft speed with constant IGV angle.

Using IGV angle and shaft speed it is possible to implement adaptive model-based prediction schemes which produce smooth yet unlagged estimates of air speed and volumetric flow rate.

6 Validation of air mass flow rate

The primary means of validating the air mass flow rate is to perform a real-time mass balance using the fuel gas mass flow rate in order to predict the exhaust gas oxygen concentration (% vol) measured by the unit's existing emissions monitoring system [6]. Typically it is possible to predict this variable value within 0.15 % vol for 95% of the time during steady state operation.

Secondary validation is possible with a real-time energy balance – provided that good estimates are available for cooled extraction air flows from the compressor – by predicting the turbine exhaust gas temperature. It is usually possible to predict this temperature to within 5 °C for 95% of the time during steady state operation.

Both of these validation methods require an accurate (< 0.5% of reading) fuel gas mass flow rate measurement and real-time fuel gas composition data from an online gas chromatograph.

Figure 6 shows an example of these two validation methods applied to a W501G gas turbine (with compressor upgrade) operating at base load. The scattered points represent the raw air mass flow rate readings from the system and the solid line is a smoothed estimate. The random uncertainty is computed from the standard deviation of the differences between the raw and the smooth signals. Average air density and mass flow rate during this time interval were 1.181 kg/m^3 and 576.6 kg/s respectively.

The root-mean-square (rms) values for the prediction errors of exhaust gas oxygen content and exhaust gas temperature are also displayed on the chart. On this particular gas turbine, all

turbine cooling air flows were measured directly and hence the accuracy of the exhaust gas temperature prediction. The mass flow rate is using the duct factor derived from the CFD simulation runs, which is 0.985 for this load.

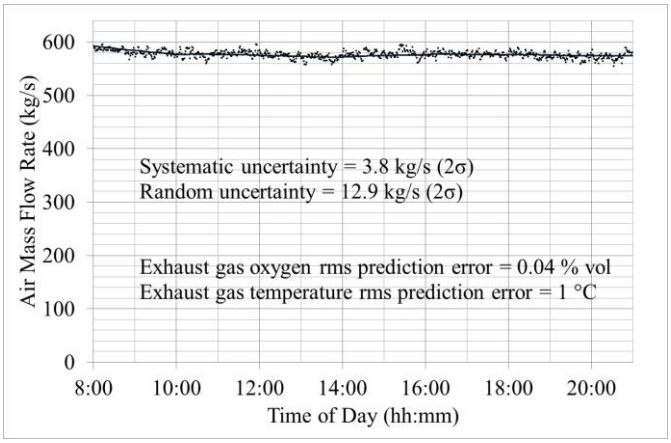

Figure 6: W501G with compressor upgrade at base load

7 Discussion of experiences

Two main types of benefit are derived from the installed systems: (a) regularly occurring benefits from more accurate real-time and day-ahead load forecasting which permits the power generation companies to maximize the cash flow for the combined cycle units to which the gas turbines belong and (b) opportunistic benefits arising from when the air mass flow rate measurement provides reliable early warning of potentially damaging plant issues.

This section provides a selection of incidents from the second category where the extra information provided by the ultrasonic air mass flow rate measurement has made a significant contribution to understanding or solving gas turbine performance issues.

7.1 Compressor upgrade before/after comparison

The ultrasonic flow measurement system has been in place on the same gas turbine before and after a compressor upgrade. Following return to service, the increase in volumetric flow rate at full IGV opening, from 445 to 476 m^3/s, was immediately evident and quickly quantifiable (+7.0%).

7.2 Compressor bleed valve seals leaking

On two nominally identical gas turbines in the same combined cycle unit, the generator power outputs had been significantly different (3%) at base load for many months. Following installation of the mass flow rate measurement, the base load air mass flow rates were in close agreement, although the real-time energy balances from the two turbines suggested that less air was entering the combustion chambers in the underperforming turbine. This information was used to focus further tests on the compressor bleed valves, and in a subsequent inspection it was found that the seals had degraded on the high and low pressure bleed valves on the underperforming turbine. Repair of the seals reduced the performance difference between the two turbines.

7.3 Compressor bleed valve stuck open after start-up

Following the start-up of a gas turbine, generator power output was lower than expected. The relationship between IGV angle and volumetric flow rate remained unchanged, but the relationship between IGV angle and compressor normalized pressure ratio had changed, and the actual normalized pressure ratio value of 15.6 was lower than expected value of 16.1. This suggested that the normal amount of air was entering the compressor, but that the discharge flow rate from the compressor was lower than normal. This information lead to the root cause being quickly determined, and power output restored.

7.4 Compressor failure diagnosis and prevention

An upgraded compressor had failed catastrophically twice within 12 months. The ultrasonic mass flow rate measurement was installed after the second failure. The data from the flowmeter, when related to existing plant signals, indicated that the failures were unlikely to have been surge events, as had been suspected, but were more likely to have been caused by overheating of the final compressor stages. Based upon this information, a compressor monitoring algorithm was designed and implemented and recurrence of the failure has been avoided in the three years since.

7.5 Early warning of turbine vane damage

The accurate measurement of air mass flow rate allows turbine inlet temperature to be estimated to greater accuracy and hence a useful real-time turbine (expander) isentropic efficiency metric to be computed. With this metric in place, a sudden drop of 1.5% was observed in turbine efficiency after some large and rapid load changes, and subsequent to this event the engine was unable to reach full power output. Changes in cooling air flows corroborated the efficiency drop and the unit was shut down for borescope inspection which revealed significant damage in second stage turbine vanes.

7.6 Reversed heat exchangers in inlet air cooler

On a gas turbine with a three port air intake filter house, newly installed inlet air cooling coils in the three ports were causing a significant change in the air flow angle measured by the ultrasonic probes when the cooling water was admitted through the coils. The consistent change in average air flow angle, θ, in the trapezoidal section, from +9° to +5°, suggested that the cooling contribution of the three ports was not balanced. It was subsequently found that on one of the side ports the supply and return cooling water lines had been wrongly connected and thus the designed counter-flow was not implemented. The pipework was corrected and the air flow angle then remained relatively unchanged by inlet cooling.

8 Conclusions and future development

The measurement of air mass flow rate in a gas turbine intake duct using the ultrasonic time-of-flight principle presents particular challenges because of the geometries of the ducts and the high levels of noise, vibration and turbulence, but these can be overcome with careful design and selection of appropriate signal processing techniques.

The accuracy of the measurement depends upon the duct geometry and the air flow rates, and in the 28 applications to date, uncertainty analyses have indicated systematic uncertainties in the range 0.5 to 2.0% of reading at base load.

The regular benefits of the systems come from improved load forecasting for the gas turbine and the associated combined cycle unit, and opportunistic benefits from faster diagnosis of performance issues and early warnings of potentially serious damage.

The future development plans are for lower cost multiple plane systems which can be quickly and easily installed and therefore reduce the reliance on the CFD simulations, which can often be the most time-consuming part of the project.

Acknowledgements

Real Time Power acknowledges the technical assistance and input provided by our customers in the installation and operation of the ultrasonic air mass flow rate systems.

References

[1] American Society of Mechanical Engineers. “ASME PTC 19.5-2004 Flow Measurement Performance Test Codes”, pp. 113-123, (2004).

[2] G.J. Van Wylen, R.E. Sonntag, “Fundamentals of Classical Thermodynamics”, p. 599, 2nd Edition, Wiley, (1978).

[3] http://ptd.leica-geosystems.com/downloads123/cp/disto/3DDisto/manuals/Leica_3D_Disto_UserManual_en.pdf, (2015).

[4] R. R. Gay, C. A. Palmer, M. R. Erbes. “Power Plant Performance Monitoring”, pp. 110-116, R-Squared (2004).

[5] http://resource.npl.co.uk/acoustics/techguides/speedair, (2015).

[6] American Society of Mechanical Engineers. “ASME PTC 22-2005 Gas Turbine Performance Test Codes”, pp. 56-75, (2005).